Geomechanics and Engineering, *Vol. 21, No. 5 (2020) 447-459*
DOI: https://doi.org/10.12989/gae.2020.21.5.447

Micropolar thermoelastic medium with voids under the effect of rotation concerned with 3PHL model

Mohamed I. A. Othman*[1], Amnah M. Alharbi[2a] and Al-Anoud M. Kh. Al-Autabi[2b]

[1]*Department of Mathematics, Faculty of Science, Zagazig University,P.O. Box 44519, Zagazig, Egypt*
[2]*Department of Mathematics, Faculty of Science, Taif University, Taif, Saudi Arabia*

(Received March 19, 2020, Revised April 4, 2020, Accepted April 20, 2020)

Abstract. This paper aims to investigate the effect of rotation on a micropolar thermoelastic medium with voids problem. The problem is assessed according to three-phase-lag model. The normal mode analysis used to obtain the analytical expressions of the considered variables. The non-dimensional displacement, temperature, Micro rotation, the change in the volume fraction field, and stress of the material are obtained and illustrated graphically. Comparisons are made with the results predicted by two theories; namely three- phase-lag model (3PHL) and Green-Naghdi theory of type III (G-N III). The considered variables were plotted for different values of the rotation parameter, the phase-lag of heat flux and the phase-lag of temperature. The numerical results reveal that the rotation and the phase-lag times significantly influence the distribution of the field quantities. Some particular cases of interest are deduced from the present investigation.

Keywords: micropolar; voids; rotation; Green-Naghdi theory; three-phase-lag

1. Introduction

The theory of micropolar materials has been found to be useful when working with a class of substances that demonstrate particular microscopic effects arising from the local system and the micro-motions of the media. The linear theory of micropolar elasticity has been found to be a sufficient principle to stand for the behavior of such materials. In the case of ultrasonic waves, such as the elastic vibrations that are differentiated by high frequencies and minute wavelengths, the effects of the body microstructure become considerable. The established effects of micro-structure lead to the advancement of fresh forms of waves that are not included in the classical theory elasticity. Materials such as composites, metals, soils, polymers, concrete, and rocks are distinctive media with micro-structures. In general terms, the majority of artificial and natural materials such as geological, engineering, and bio-logical media have micro-structures. The developers of the linear theory of micropolar elasticity (Eringen, 1966 and Eringen, 1970) viewed the principle as a theory of couple stress.

Marin (1998, 2016, and 2017) explained various types of challenges in the concept of micro-polar of elastic solid with negations. The concept of linear elastic materials with negations is among the most crucial generalizations of the conventional principle of elasticity. This concept has been found to be critical in the assessment of different types of biological and geological elements in which the elastic principle is sufficient. This hypothesis focuses on elastic materials that consist of a distribution of minute porous (voids), in which the small porous' volume is incorporated among the kinetics changeable, and in the restricting case of evaporating this volume; it decreases to the traditional concept of elasticity. The principle of thermoelastic elements with voids and with limited energy of indulgence was initiated by Cicco and Diaco (2002). In addition, Puri and Cowin (1985) explored the characteristics of plane waves in a linear elastic component with small porous (voids). In 1986, Iesan demonstrated a linear concept for a thermoelastic element with voids. Iesan developed the primary equations and demonstrated the exceptionality of the solution, reciprocity connection, and variation description of the solution in the dynamical principle. Hobiny and Abbas (2020) described the fractional-order thermoelastic wave survey in two different mediums that consisted of small porous.

According to Nunziato and Cowin (1979), waves are in rotational elastic solid with voids. Dhaliwal and Wang (1994) discussed the sphere of influence concept in the linear principle of elastic elements with voids. Scarpetta (1995), on the other hand, explored the good posedness assumptions of linear elastic components with voids. Additionally, Kaddari *et al.* (2020) initiated research on the structural behavior of the functionality of the graded porous plates based on elastic knowledge by exploiting a new quasi-3D mode. Equally, Arifa *et al.* (2017) investigated the characteristics of plane harmonic waves subjected in a rotational medium under the influence of micro-temperature

*Corresponding author, Professor
E-mail: m_i_a_othman@yahoo.com
[a]Ph.D.
E-mail: alharbi.a.m@hotmail.com
[b]Ph.D.
E-mail: do_dey@windowslive.com

ISSN: 2005-307X (Print), 2092-6219 (Online)

and double-phase-lag thermoelasticity. The influence of inclined load and hall current in diagonally isotropic magneto-thermoelastic revolving medium with the order of functionality promotes heat transmission due to the normal force (Lata and Kaur 2018a, b). Al-Basyouni *et al.* (2020) carried out an investigation that focused on the influence of revolving on the thermal stress wave conveyed in a non-homogenous viscoelastic medium. Lata and Singh (2019) examined the implication of nonlocal factor on nonlocal thermoelastic rock subjected to an inclined load.

Abo-Dahab *et al.* (2019), on the other hand, explored the influence of gravity and revolving on an electro-magneto-thermoelastic object with both voids and diffusion through dual-phase-lag and Lord-Shulman models. Mirzaei *et al.* (2019) conducted a steady-state analysis to examine the creep evaluation of rotating functionality that was graded by a plain blade. Abbas and Marin (2017) also assessed the systematic solution of thermoelastic association in a half-space using the pulsed laser heater. Explanation regarding the partition of energies was provided by Marin *et al.* (2019). In this case, the authors indicated that the energy for the backward time is an issue of thermoelastic components with a dipolar system. The severity of complex circular plates by radial ribs was enhanced by Itu *et al.* (2019). Ellahi *et al.* (2018) explored the effects of a shiny film coating on different fluid flows of revolving disks balanced with nano-sized gold and silver particles. Thermally established peristaltic propulsion of magnetic object components in bioarchaeological liquids was studied by Bhatti *et al.* (2018). In addition, Shahid *et al.* (2020) demonstrated the mathematical assessment of the swimming of gyrotactic micro-organisms in none liquids through absorbent objects over an outlined facade. The activation energy for the transfer of gyrostatic micro-organisms in the magnetized none liquids and how they pass through a porous place was examined by Bhatti *et al.* (2020).

A three-phase-lag formulation of the linearized principle of dual-thermoelasticity was created based on the heat law considerations that included the thermal displacement and temperature gradient as among the constitutive factors. Estimation to an alteration of the Fourier law with three distinctive transformations for the heat flux vector, for the thermal displacement gradient as well as for the temperature gradient replaced the existing Fourier law. The generalization of the dual concept of thermoelasticity was generated by Chandrasekharaiah (1987) and Tzau (1995) and was referred to as the double phase-lag thermoelasticity model. Tzou (1995) took into account the micro-structural influence in the delayed reaction in time in the microscopic model that is created by considering the amplification of the lattice temperature that was held up due to phonon-electron associations of the macroscopic stage. In this case, a macroscopic lagging reaction between the heat flux and temperature gradient appeared to be a potential result based on the progressive interactions. However, Tzou (1995) established a two-phase lagging model for both temperature gradient and heat flux vector. The author took to account the constitutive equations that assist in explaining the lagging behavior in heat transfer in solid materials. Lately, Roy Choudhuri (2007) introduced a more generalized numerical formulation for a double thermoelasticity principle that involves a three-phase lagging variable including Thermo displacement gradient, temperature gradient as well as heat flux vector. This formulation was developed by reducing the previous model to suit particular cases. This specialized formulation indicated that heat flux is transformed as

$\boldsymbol{q}(p,t+\tau_q) = -[K\nabla T(p,t+\tau_\theta) + K^*\nabla\nu(p,t+\tau_\nu)$ where K^* stands for the additional material constant and $\nabla\nu$ $(\dot{\nu}=T)$ represents the thermal displacement gradient. The developed equation provides considerably different outcomes when used to examine some pertinent, applicable issues, particularly those challenges associated with heat movement, short and high heat fluxes. In such a case, the hyperbolic equation suggests that the lagging characteristics in heat transfer in solid materials should not be under-estimated. It is worth noting that three-phase-lag formulation is critical is assessing issues related to exo-thermic catalytic responses, nuclear boiling, and phonon-scattering and phonon-electron interactions among others where the delay period τ_q helps to include the thermal wave conduct. In addition, the phase-lag τ_θ helps to obtain the influence of phonon-electron interactions. The other delay period τ_ν is efficient since it makes the thermal displacement gradient to be examined as a constitutive factor. Sur and Kanoria (2014, 2015) and Othman *et al.* (2015, 2017, and 2019), explained the main problems associated with the three-phase-lag model and the issues connected to the concept of micropolar thermo-elasticity. Accordingly, Othman *et al.* (2014) outlined the influence of revolving and original stress on a generalized micropolar thermoelastic object with the three-phase lagging model.

The current study objects to examine the influence of revolving on isotropic, homogeneous, the thermally micropolar elastic object will small porous according to the 3PHL formulation and thermoelasticity with energy dissipation (G-N III) principle. The results of the analysis were acquired by employing normal mode evaluation. The results were also compared with the three principles in the absence and presence of rotation and two distinctive values of relaxation periods. The circulations of all the targeted variables were graphically represented.

2. Formulation of the problem

We consider a homogeneous and micropolar thermo-elastic medium with voids rotating uniformly with angular velocity $\boldsymbol{\Omega} = \Omega\boldsymbol{n}$, where $\boldsymbol{n}$ is a unit vector representing the direction of the axis of rotation. Schoenberg and Censor (1973) show that, the displacement equation of motion in the rotating frame has two additional terms: the centripetal acceleration $\boldsymbol{\Omega}\times(\boldsymbol{\Omega}\times\boldsymbol{u})$ due to the time-varying motion only and the Coriolis acceleration $2(\boldsymbol{\Omega}\times\dot{\boldsymbol{u}})$ where $\boldsymbol{u}=(u,0,w)$ is the dynamic displacement vector, the micro-rotation vector is $\boldsymbol{\phi}=(0,\phi_2,0)$ and $\boldsymbol{\Omega}=(0,\Omega,0)$ is the angular velocity. We take the rectangular Cartesian coordinates with the origin on the surface y=0 and z-axis normally into the medium, which is represented by z≥0. If

we restrict our analysis parallel to *xz*- plane.

2.1 Constitutive relations: (El-Karamany and Ezzat 2013)

$$\sigma_{ij} = 2\,\mu\varepsilon_{ij} + k(u_{j,i} - \varepsilon_{ijr}\varphi_r) + (\lambda e + \beta^* \psi - \upsilon T)\delta_{ij}, \quad (1)$$

$$m_{ij} = \alpha\varphi_{r,r}\,\delta_{ij} + \beta\varphi_{i,j} + \gamma\varphi_{j,i}, \quad (2)$$

$$\varepsilon_{ij} = \frac{1}{2}(u_{i,j} + u_{j,i}). \quad (3)$$

2.2 Equation of motion: (Othman et al. 2015)

$$\sigma_{ji,j} = \rho[\ddot{u}_i + \{\boldsymbol{\Omega}\times(\boldsymbol{\Omega}\times\mathbf{u})\}_i + 2(\boldsymbol{\Omega}\times\dot{\mathbf{u}})_i]. \quad (4)$$

Using Eqs. (1) and (3), Eq. (4) can be written as:

$$\begin{aligned}(\mu+k)\nabla^2 u_i + (\lambda+\mu)e_{,i} + k(\nabla\times\boldsymbol{\varphi})_{,i} + \beta^*\psi_{,i} - \upsilon T_{,i} \\ = \rho[\ddot{u}_i + \{\boldsymbol{\Omega}\times(\boldsymbol{\Omega}\times\mathbf{u})\}_i + 2(\boldsymbol{\Omega}\times\dot{\mathbf{u}})_i].\end{aligned} \quad (5)$$

2.3 Heat conduction equation with 3PHL model (Choudhuri 2007)

$$\begin{aligned}K^*(1+\tau_\nu\frac{\partial}{\partial t})\nabla^2 T + K(1+\tau_\theta\frac{\partial}{\partial t})\nabla^2\dot{T} = (1+\tau_q\frac{\partial}{\partial t} \\ + \frac{1}{2}\tau_q^2\frac{\partial^2}{\partial t^2})(\rho C_e\ddot{T} + \upsilon T_0\ddot{e} + mT_0\frac{\partial\psi}{\partial t}).\end{aligned} \quad (6)$$

2.4 Micropolar equation

$$\varepsilon_{ijp}\,\sigma_{jp} + m_{ji,j} = \rho j[\ddot{\varphi}_i + (\boldsymbol{\Omega}\times\dot{\boldsymbol{\varphi}})_i]. \quad (7)$$

Using Eqs. (1) – (3), Eq. (7) take the form:

$$\begin{aligned}(\alpha+\beta+\gamma)\nabla(\nabla.\boldsymbol{\varphi})_i - \gamma\nabla\times(\nabla\times\boldsymbol{\varphi})_i + k(\nabla\times\boldsymbol{u})_i \\ - 2k\,\boldsymbol{\varphi}_i = \rho j\,[\ddot{\varphi}_i + (\boldsymbol{\Omega}\times\dot{\boldsymbol{\varphi}})_i].\end{aligned} \quad (8)$$

2.5 Voids equation

$$\alpha^*\nabla^2\psi - \eta^*\psi - \omega^*\frac{\partial\psi}{\partial t} - \beta^* e + mT = \rho\,\zeta^*\ddot{\psi}. \quad (9)$$

Then, the governing equations for a micropolar thermoelastic medium with voids under the effect of a rotation with 3PHL model can be rewritten as,

$$(\mu+k)\nabla^2 u + (\lambda+\mu)e_{,x} - k\phi_{2,z} + \beta^*\psi_{,x} - \upsilon T_{,x} = \rho[\ddot{u} - \Omega^2 u + 2\Omega\dot{w}], \quad (10)$$

$$(\mu+k)\nabla^2 w + (\lambda+\mu)e_{,z} + k\phi_{2,x} + \beta^*\psi_{,z} - \upsilon T_{,z} = \rho[\ddot{w} - \Omega^2 w - 2\Omega\dot{u}], \quad (11)$$

$$K^*(1+\tau_\nu\frac{\partial}{\partial t})\nabla^2 T + K(1+\tau_\theta\frac{\partial}{\partial t})\nabla^2\dot{T}$$

$$= (1+\tau_q\frac{\partial}{\partial t} + \frac{1}{2}\tau_q^2\frac{\partial^2}{\partial t^2})(\rho C_e\ddot{T} + \upsilon T_0\ddot{e} + mT_0\frac{\partial\psi}{\partial t}). \quad (12)$$

$$\gamma\nabla^2\varphi_2 + k(\frac{\partial u}{\partial z} - \frac{\partial w}{\partial x}) - 2k\phi_2 = \rho j\ddot{\phi}_2, \quad (13)$$

$$\alpha^*\nabla^2\psi - \eta^*\psi - \omega^*\frac{\partial\psi}{\partial t} - \beta^* e + mT = \rho\zeta^*\ddot{\psi}. \quad (14)$$

Also, the stress tensor and couple stress tensor components take the form:

$$\sigma_{xx} = (2\mu+k)u_{,x} + \lambda e + \beta^*\psi - \upsilon T, \quad (15)$$

$$\sigma_{yy} = \lambda e + \beta^*\psi - \upsilon T, \quad (16)$$

$$\sigma_{zz} = (2\mu+k)w_{,z} + \lambda e + \beta^*\psi - \upsilon T, \quad (17)$$

$$\sigma_{xz} = \mu u_{,z} + (\mu+k)w_{,x} + k\phi_2, \quad (18)$$

$$\sigma_{zx} = (\mu+k)u_{,z} + \mu w_{,x} - k\phi_2, \quad (19)$$

$$m_{xy} = \gamma\frac{\partial\phi_2}{\partial x}, \quad (20)$$

$$m_{yx} = \beta\frac{\partial\phi_2}{\partial x}, \quad (21)$$

$$m_{yz} = \beta\frac{\partial\phi_2}{\partial z}, \quad (22)$$

$$m_{zy} = \gamma\frac{\partial\phi_2}{\partial z}, \quad (23)$$

$$m_{xx} = m_{yy} = m_{zz} = m_{xz} = m_{zx} = 0. \quad (24)$$

For simplifications we shall use the following non-dimensional variables

$$\begin{aligned}\{x', z'\} = \frac{\omega}{c_1}\{x, z\},\ \{u', w'\} = \frac{\rho\omega c_1}{\upsilon T_0}\{u, w\},\ \sigma_{ij}' = \frac{\sigma_{ij}}{\upsilon T_0}, \\ \{t', \tau_\theta', \tau_q'\} = \omega\{t, \tau_\theta, \tau_q\},\quad \{\phi_2', \psi'\} = \frac{\rho c_1^2}{\upsilon T_0}\{\phi_2, \psi\}, \\ m_{ij}' = \frac{\omega}{c_1\upsilon T_0}m_{ij}.\quad \Omega' = \frac{\Omega}{\omega},\quad T' = \frac{T}{T_0},\end{aligned} \quad (25)$$

where $c_1^2 = \dfrac{(\lambda+2\mu+k)}{\rho}$ and $\omega = \dfrac{\rho C_e c_1^2}{K^*}$.

Using (25), governing Eqs. (10)-(14), become

$$\begin{aligned}(\frac{\mu+k}{\rho c_1^2})\nabla^2 u + (\frac{\lambda+\mu}{\rho c_1^2})e_{,x} - (\frac{k}{\rho c_1^2})\phi_{2,z} + (\frac{\beta^*}{\rho c_1^2})\psi_{,x} \\ -T_{,x} = [\ddot{u} - \Omega^2 u + 2\Omega\dot{w}],\end{aligned} \quad (26)$$

$$(\frac{\mu+k}{\rho c_1^2})\nabla^2 w+(\frac{\lambda+\mu}{\rho c_1^2})e_{,z}+(\frac{k}{\rho c_1^2})\phi_{2,x}+(\frac{\beta^*}{\rho c_1^2})\psi_{,z} -T_{,z}=[\ddot{w}-\Omega^2 w-2\Omega\dot{u}], \tag{27}$$

$$K^*(1+\tau_v\frac{\partial}{\partial t})\nabla^2 T+K\omega(1+\tau_\theta\frac{\partial}{\partial t})\nabla^2\dot{T}=(1+\tau_q\frac{\partial}{\partial t} +\frac{1}{2}\tau_q^2\frac{\partial^2}{\partial t^2})(\rho C_e c_1^2\frac{\partial^2 T}{\partial t^2}+\frac{\upsilon^2 T_0}{\rho}\frac{\partial^2 e}{\partial t^2}+\frac{m\upsilon T_0}{\rho\omega}\frac{\partial\psi}{\partial t}), \tag{28}$$

$$[\nabla^2-(\frac{\rho j c_1^2}{\gamma})\frac{\partial^2}{\partial t^2}-2\frac{k c_1^2}{\gamma\omega^2}]\phi_2+\frac{k c_1^2}{\gamma\omega^2}(\frac{\partial u}{\partial z}-\frac{\partial w}{\partial x})=0, \tag{29}$$

$$[\nabla^2-(\frac{\rho\zeta^* c_1^2}{\alpha^*})\frac{\partial^2}{\partial t^2}-(\frac{\omega^* c_1^2}{\alpha^*\omega})\frac{\partial}{\partial t}-\frac{\eta^* c_1^2}{\alpha^*\omega^2}]\psi -(\frac{\beta^* c_1^2}{\alpha^*\omega^2})e+(\frac{m\rho c_1^4}{\alpha^*\omega^2\upsilon})T=0. \tag{30}$$

Also, the stress tensor components (15)-(19), using (25), become

$$\sigma_{xx}=(\frac{2\mu+k}{\rho c_1^2})u_{,x}+(\frac{\lambda}{\rho c_1^2})e+(\frac{\beta^*}{\rho c_1^2})\psi-T, \tag{31}$$

$$\sigma_{yy}=(\frac{\lambda}{\rho c_1^2})e+(\frac{\beta^*}{\rho c_1^2})\psi-T, \tag{32}$$

$$\sigma_{zz}=(\frac{2\mu+k}{\rho c_1^2})w_{,z}+(\frac{\lambda}{\rho c_1^2})e+(\frac{\beta^*}{\rho c_1^2})\psi-T, \tag{33}$$

$$\sigma_{xz}=(\frac{\mu}{\rho c_1^2})u_{,z}+(\frac{\mu+k}{\rho c_1^2})w_{,x}+(\frac{k}{\rho c_1^2})\phi_2, \tag{34}$$

$$\sigma_{zx}=(\frac{\mu+k}{\rho c_1^2})u_{,z}+(\frac{\mu}{\rho c_1^2})w_{,x}-(\frac{k}{\rho c_1^2})\phi_2. \tag{35}$$

Similarly, the couple stress tensor components (20)-(23), using (25), take the form

$$m_{xy}=(\frac{\gamma\omega^2}{\rho c_1^4})\frac{\partial\phi_2}{\partial x}, \tag{36}$$

$$m_{zy}=(\frac{\gamma\omega^2}{\rho c_1^4})\frac{\partial\phi_2}{\partial z}, \tag{37}$$

$$m_{yx}=(\frac{\beta\omega^2}{\rho c_1^4})\frac{\partial\phi_2}{\partial x}, \tag{38}$$

$$m_{yz}=(\frac{\beta\omega^2}{\rho c_1^4})\frac{\partial\phi_2}{\partial z}. \tag{39}$$

We introduce the displacement potentials $q_1(x,z,t)$ and $q_2(x,z,t)$ which are related to displacement components as

$$\text{Let}\quad u=q_{1,x}+q_{2,z},\quad w=q_{1,z}-q_{2,x}. \tag{40}$$

Using (40), Eqs. (26)-(30), become:

$$[\nabla^2-\frac{\partial^2}{\partial t^2}+\Omega^2]q_1+2\Omega\frac{\partial q_2}{\partial t}-T+(\frac{\beta^*}{\rho c_1^2})\psi=0, \tag{41}$$

$$-2\Omega\frac{\partial q_1}{\partial t}+[(\frac{\mu+k}{\rho c_1^2})\nabla^2-\frac{\partial^2}{\partial t^2}+\Omega^2]q_2-(\frac{k}{\rho c_1^2})\phi_2=0, \tag{42}$$

$$K^*(1+\tau_v\frac{\partial}{\partial t})\nabla^2 T+K\omega(1+\tau_\theta\frac{\partial}{\partial t})\nabla^2\dot{T}=(1+\tau_q\frac{\partial}{\partial t} +\frac{1}{2}\tau_q^2\frac{\partial^2}{\partial t^2})(\rho C_e c_1^2\ddot{T}+\frac{\upsilon^2 T_0}{\rho}\nabla^2\ddot{q}_1+\frac{m\upsilon T_0}{\rho\omega}\frac{\partial\psi}{\partial t}), \tag{43}$$

$$[\nabla^2-(\frac{\rho j c_1^2}{\gamma})\frac{\partial^2}{\partial t^2}-2\frac{k c_1^2}{\gamma\omega^2}]\phi_2+\frac{k c_1^2}{\gamma\omega^2}\nabla^2 q_2=0, \tag{44}$$

$$[\nabla^2-(\frac{\rho\zeta^* c_1^2}{\alpha^*})\frac{\partial^2}{\partial t^2}-(\frac{\omega^* c_1^2}{\alpha^*\omega})\frac{\partial}{\partial t}-\frac{\eta^* c_1^2}{\alpha^*\omega^2}]\psi-(\frac{\beta^* c_1^4}{\alpha^*\omega^4})\nabla^2 q_1+(\frac{m\rho c_1^4}{\alpha^*\omega^2\upsilon})T=0. \tag{45}$$

3. Normal mode analysis

The solution of the considered physical variable can be decomposed in terms of normal modes as the following from:

$$[u,w,q_1,q_2,T,\phi_2,\psi,\sigma_{ij}](x,z,t) =[u^*,w^*,q_1^*,q_2^*,T^*,\phi_2^*,\psi^*,\sigma_{ij}^*](z)e^{st+iax}, \tag{46}$$

where s is the complex time constant, a is the wave number in the x-direction and u^*, w^*, q_1^*, q_2^*,T^*, ϕ_2^*, are ψ^*, σ_{ij}^* the amplitudes of the functions u,w, q_1, q_2, T, ϕ_2, ψ, σ_{ij}.

Using Eq. (46) then, Eqs. (41)-(45) take form:

$$[D^2-b_1]q_1^*+b_2 q_2^*-T^*+a_1\psi^*=0, \tag{47}$$

$$[a_2 D^2-b_3]q_2^*-b_2 q_1^*-a_3\phi_2^*=0, \tag{48}$$

$$[b_4 D^2-b_5]T^*-[b_6 D^2-b_7]q_1^*-b_8\psi^*=0, \tag{49}$$

$$[D^2-b_9]\phi_2^*+[a_{11}D^2-b_{10}]q_2^*=0, \tag{50}$$

$$[D^2-b_{11}]\psi^*-[a_{15}D^2-b_{12}]q_1^*+a_{16}T^*=0. \tag{51}$$

Eliminating q_1^*, q_2^*, T^*, ϕ_2^*, ψ^* between Eqs. (47)-

(51) we obtain

$$(\mathrm{D}^{10}-A\,\mathrm{D}^{8}+B\,\mathrm{D}^{6}-C\,\mathrm{D}^{4}+E\,\mathrm{D}^{2}-F)(q_1^*,q_2^*,T^*,\phi_2^*,\psi^*)=0. \quad (52)$$

The solution of Eqs. (52) - (56) are given by

$$(q_1^*,q_2^*,T^*,\phi_2^*,\psi^*)(\mathrm{z})=\sum_{n=1}^{5}(1,H_{1n},H_{2n},H_{3n},H_{4n})M_n e^{-k_n z}, \quad n=1,2,3,4,5 \quad (53)$$

where M_n is some constant and $k_n^2,(n=1,2,3,4,5)$ are the roots of the characteristic equation of Eq. (52).

In order to obtain the displacement components u, w using Eqs. (46) and (53) into Eq. (40), respectively, we get

$$w^*=-\sum_{n=1}^{5}[k_n+iaH_{1n}]M_n e^{-k_n z}, \quad (54)$$

$$u^*=\sum_{n=1}^{5}[ia-k_n H_{1n}]e^{-k_n z}. \quad (55)$$

The stresses components are

$$\sigma_{xx}^*=\sum_{n=1}^{5}[-a_{17}(a^2+iak_nH_{1n})+a_{18}(k_n^2-a^2)+a_1H_{4n}-H_{2n}]M_n e^{-k_n z}, \quad (56)$$

$$\sigma_{yy}^*=\sum_{n=1}^{5}[a_{18}(k_n^2-a^2)+a_1H_{4n}-H_{2n}]M_n e^{-k_n z}, \quad (57)$$

$$\sigma_{xz}^*=\sum_{n=1}^{5}[a_{19}k_n^2H_{1n}-ia(a_2+a_{19})k_n+a_2a^2H_{1n}+a_3H_{3n}]M_n e^{-k_n z}, \quad (58)$$

$$\sigma_{zz}^*=\sum_{n=1}^{5}[a_{17}(k_n^2+iak_nH_{1n})+a_{18}(k_n^2-a^2)+a_1H_{4n}-H_{2n}]M_n e^{-k_n z}, \quad (59)$$

$$\sigma_{zx}^*=\sum_{n=1}^{5}[a_2k_n^2H_{1n}-ia(a_2+a_{19})k_n+a_{19}a^2H_{1n}-a_3H_{3n}]M_n e^{-k_n z}. \quad (60)$$

The micro rotation components are

$$m_{xy}^*=\sum_{n=1}^{5}iaa_{20}H_{3n}M_n e^{-k_n z}, \quad (61)$$

$$m_{zy}^*=-\sum_{n=1}^{5}a_{20}k_nH_{3n}M_n e^{-k_n z}, \quad (62)$$

$$m_{yx}^*=\sum_{n=1}^{5}iaa_{21}H_{3n}M_n e^{-k_n z}, \quad (63)$$

$$m_{yz}^*=-\sum_{n=1}^{5}a_{21}k_nH_{3n}M_n e^{-k_n z}. \quad (64)$$

where a_i, $i=1,2,3,\ldots,21$, $b_i, i=1,2,3,\ldots,12$ are given in Appendix **A** and A, B, C, E, F, H_{in}, i= 1,2,34 are given in Appendix **B**,

4. Boundary conditions

In order to determine the parameterM_1, M_2, M_3, M_4, M_5 we consider the following boundary conditions at z=0.

(1) The condition of the voids volume fraction fields constant in z direction.

$$\frac{\partial\psi}{\partial z}=0. \quad (65)$$

(2) The thermal condition the half-space subjected to thermal shock applied to the boundary. This leads to

$$T=f\,e^{st+iax}. \quad (66)$$

(3) The tangential a stress condition (stress free) then

$$\sigma_{xz}=0. \quad (67)$$

(4) The normal stress condition (mechanical stress) is constant force so that

$$\sigma_{zz}=-f_1\,\mathrm{e}^{st+iax}. \quad (68)$$

where f_1 is the magnitude of the applied force in the half-space.

(5) The couple stress tensor condition

$$m_{zy}=0. \quad (69)$$

Applying Eqs. (65)-(69) in (53), (58), (59) and (62) we get:

$$\sum_{n=1}^{5}k_nH_{8n}M_n=0, \quad (70)$$

$$\sum_{n=1}^{5}H_{2n}M_n=f, \quad (71)$$

$$\sum_{n=1}^{5}S_{3n}M_n=0, \quad (72)$$

$$\sum_{n=1}^{5}S_{4n}M_n=-f_1, \quad (73)$$

$$\sum_{n=1}^{5}S_{4n}M_n=0. \quad (74)$$

After applying the inverse of matrix method for the above equations, the values of the constants $M_{\mathrm{n}}(\mathrm{n}=1,2,3,4,5)$ can be obtained by using the Matlab

program.

$$\begin{pmatrix} M_1 \\ M_2 \\ M_3 \\ M_4 \\ M_5 \end{pmatrix} = \begin{pmatrix} k_1H_{41} & k_2H_{42} & k_3H_{43} & k_4H_{44} & k_5H_{45} \\ H_{21} & H_{22} & H_{23} & H_{24} & H_{25} \\ S_{31} & S_{32} & S_{33} & S_{34} & S_{35} \\ S_{41} & S_{42} & S_{43} & S_{44} & S_{45} \\ S_{71} & S_{72} & S_{73} & S_{74} & S_{75} \end{pmatrix}^{-1} \begin{pmatrix} 0 \\ f \\ 0 \\ -f_1 \\ 0 \end{pmatrix}. \quad (75)$$

where $S_{ji}, j=1,2,3,\ldots,9$ are given in Appendix **B**.

Hence; the expressions of displacements, stresses, temperature distribution, micro-rotation and the change in the volume fraction field of micropolar generalized thermoelastic medium with voids in the present of rotation in the context of three-phase-lag theory of thermoelasticity also, can be obtained.

5. Particular and special cases of thermoelastic theory

We discuss some special cases for different values of the parameters considered in the problem.

5.1 Equations of the 3PHL model

When $\tau_v, \tau_\theta, \tau_q > 0$, $K^*, K > 0,$ and the solutions are always (exponentially) stable if $\frac{2K\tau_\theta}{\tau_q} > \tau_\upsilon^* > K^*\tau_q$ as in Quintanilla and Racke (2008).

5.2 Equations of the thermoelasticity with energy dissipation (G-N III) theory

When, $K^* \neq 0, \quad K \neq 0, \quad \tau_\theta = \tau_\upsilon = \tau_q = 0.$

6. Numerical results and discussions

Suppose that the medium is a magnesium crystal micropolar material like material subjected to mechanical and thermal disturbances for numerical calculations. The physical constant used as Othman *et al.* (2015) are

$$\mu = 4\times10^{10}\ \text{dyne/cm}^2,\ T_0 = 298\,\text{K},\ \rho = 1.74\times10^3\ \text{g/cm}^3,$$

$$\gamma = 0.779\times10^{-8}\ \text{dyne},\ \beta = 2.68*10^6,\ k = 0.85\,\text{dyne/cm}^2,$$

$$\lambda = 9.4\times10^{10}\,\text{dyne/cm}^2,\ J = 2\times10^{-20}\,\text{cm}^2,\ \varepsilon_0 = 10^{-9}/36\pi,$$

$$\mu_0 = 4\pi\times10^{-7},\ \alpha_t = 1.78\times10^{-5}\ ^{o}\text{C}.$$

The void parameters are taken as (Othman *et al.* 2015)

$$\varsigma^* = 1.475\times10^{10}\,\text{dyne/cm}^2,\quad K^* = 170\ \text{cal/cm.sec}^{o}\text{C},$$

$$\alpha^* = 3.668\times10^{-5}\,\text{dyne},\quad m = 2\times10^6\ \text{N/m}^2K,$$

$$\zeta^* = 1.753\times10^{-15}\,\text{dyne/cm}^2,\quad \omega^* = 0.0787\times10^{-3}\,\text{dyne.sec/cm}^2,$$

$$\beta^* = 1.13849\times10^{10}\,\text{dyne/cm}^2,\quad C_e = 1.04\times10^3\,\text{cal/gm}^{o}\text{C}.$$

Since, we have

$s = \zeta_1 + i\zeta_2,\ \ e^{st} = e^{\zeta_1 t}[\cos(\zeta_2 t) + i\sin(\zeta_2 t)]$ and for small values of time we can take $s = \zeta_1$ (real). The software Matlab 7.0.4 has been used to make the calculations. The computations carried out for a=0.4 m, x= 0.1 m, a= 0.4 m, x = 0.1 m, ζ_1 = 0.9 rad/s, ζ_2 = 3.7 rad/s, f=0.01, f_1=0.01 and $0 \le z \le 4$.

The comparisons have established for three cases:

(i) With two values of rotation parameter (Ω=0.18, 0.3) in the context of (G-N III) theory and (3PHL) model.

(ii) With four values of a phase-lag of the heat flux τ_q ($\tau_q = 0.3, 0.4, 0.6, 0.8$) at Ω=0.3.

(iii) With four values of a phase-lag of temperature gradient τ_θ ($\tau_\theta = 0.4, 0.5, 0.6, 0.7$) at Ω=0.3.

The computations are carried out for the non-dimensional time t=0.02 on the surface plane $x = 0.1$. The numerical technique outlined above is used for the distribution of the real part of the non-dimensional displacement w, the non-dimensional temperature T, the couple stress tensor component m_{zy} the stress components σ_{zz}, σ_{xz}, the change in the volume fraction field ψ, and the micro rotation component ϕ_2 with distance z for the problem.

6.1 The effect of rotation parameter

Figs. 1-7 show comparisons among the change in the volume fraction field ψ, the micro-rotation ϕ_2, the couple

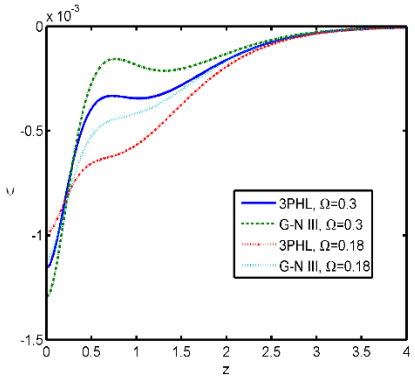

Fig. 1 Distribution of the change in the volume fraction field ψ versus z

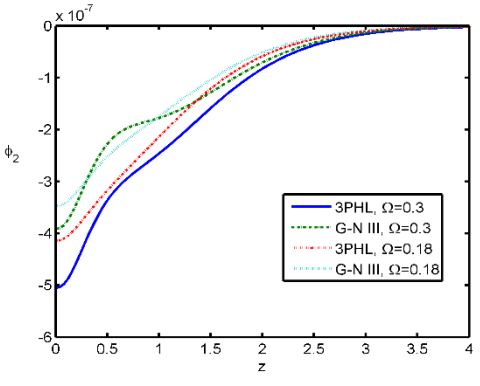

Fig. 2 Distribution of the Micro rotation component ϕ_2 versus z

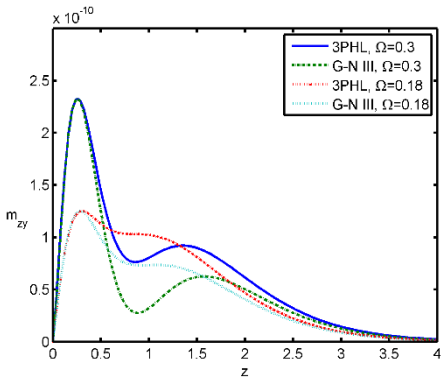

Fig. 3 Distribution of the couple stress tensor component m_{zy} versus z

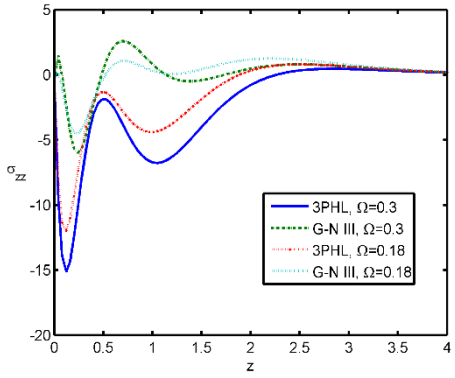

Fig. 4 Distribution of the stress component σ_{zz} versus z

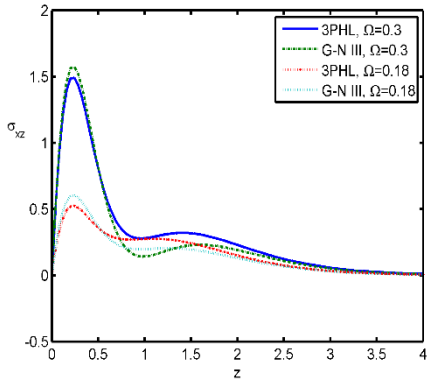

Fig. 5 Distribution of the stress component σ_{xz} versus z

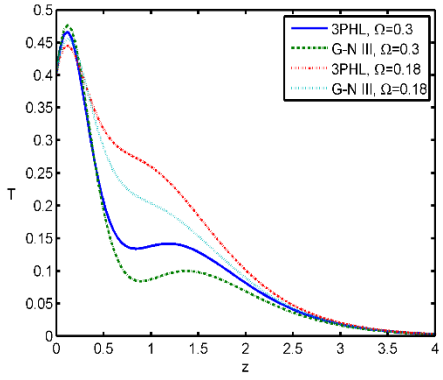

Fig. 6 Distribution of the temperature T versus z

stress m_{zy}, the force stress components σ_{zz}, σ_{xz}, the

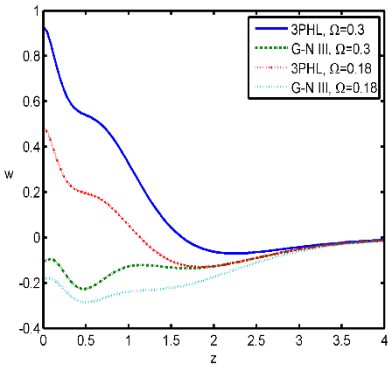

Fig. 7 Distribution of the displacement component w versus z

temperature T, and the displacement component w for different values of Ω (Ω=0.18, 0.3).

Fig. 1 explains the distribution of the change in the volume fraction field ψ against the distance z. It is noted that, the values of the change in the volume fraction field ψ for Ω=0.3 are small compared to those for Ω=0.18 in the range $0 \le z \le 0.3$; large in the range ψ, while the values are the same for two theories at $z \ge 2.5$. Fig. 2 exhibits the distribution of the micro-rotation component ϕ_2 versus z. This figure shows that, all curves start from negative values for Ω=0.18, 0.3 and the rotation parameter has a decreasing effect. In Fig. 3 the distribution of the couple stress tensor component m_{zy} begins from zero at $z = 0$ for (Ω=0.18, 0.3), which satisfy the boundary condition. It is clear that, the values of couple stress tensor component Ω=0.18 are large compared to those for Ω=0.3 for m_{zy} in the range $0 \le z \le 0.6$, but small in the range $0.6 \le z \le 1.4$; while the values are the same for the two theories when $z \ge 1.4$. Fig. 4 displays the distribution of the stress component σ_{zz} versus z. The values of stress component σ_{zz} for Ω=0.3 are small compared to those for Ω=0.18 in the range $0 \le z \le 3$, while the values are the same for the two theories when $z \ge 3$. Fig. 5 depicts the variation of the stress component σ_{xz} against the distance z, from this figure we see that, all curves begin from zero at z=0 for Ω=0.18, 0.3, which satisfy the boundary condition. The values of stress component σ_{xz} for Ω=0.3 are large compared to those for Ω=0.18 in the range $0 \le z \le 0.7$; but small in the range $0.7 \le z \le 2.5$; while the values are the same for two theories when $z \ge 2.5$. Fig. 6 exhibits the values of the temperature T against the distance z; this figure shows that, all curves start from the same value at z=0, which agree with the boundary condition. In the context of the two theories, the values of the temperature for Ω=0.3 are large compared to those for Ω=0.18 in the range $0 \le z \le 0.3$; small in the range $0.3 \le z \le 2.6$ while the values are the same for the two theories when $z \ge 2.6$. Fig. 7 displays the distribution of the displacement component w versus z. It is clear that, the rotation has an increasing effect.

6.2 The phase-lag of the heat flux effect

Figs. 8-14 show the comparisons among the change in

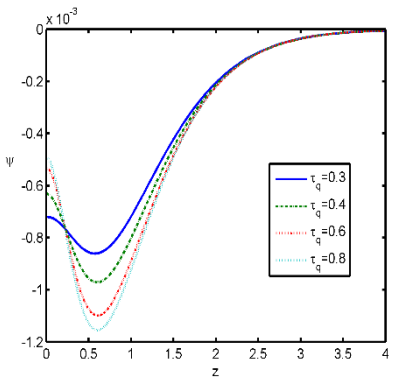

Fig. 8 Distribution of the change in the volume fraction field ψ versus z

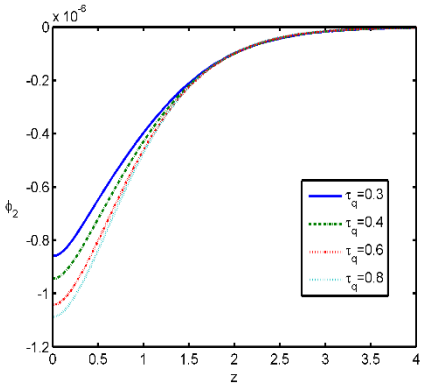

Fig. 9 Distribution of the Micro rotation component ϕ_2 versus z

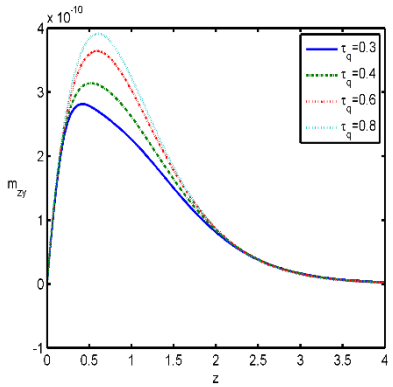

Fig. 10 Distribution of the Micro rotation component ϕ_2 versus z

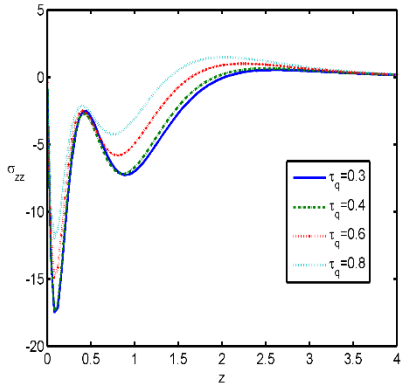

Fig. 11 Distribution of the stress component σ_{zz} versus z

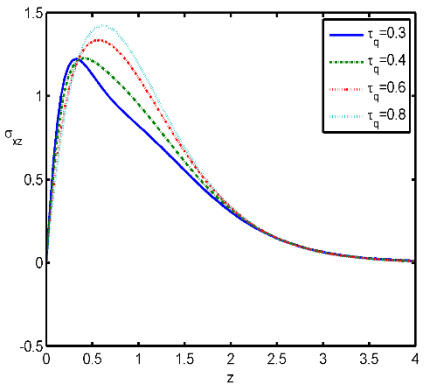

Fig. 12 Distribution of the stress component σ_{xz} versus z

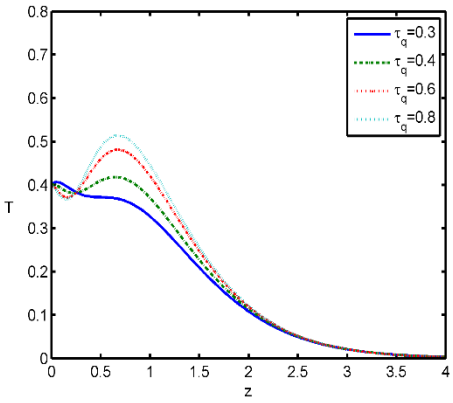

Fig. 13 Distribution of the temperature T versus z

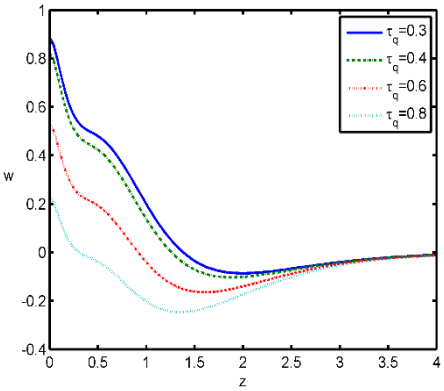

Fig. 14 Distribution of the displacement component w versus z

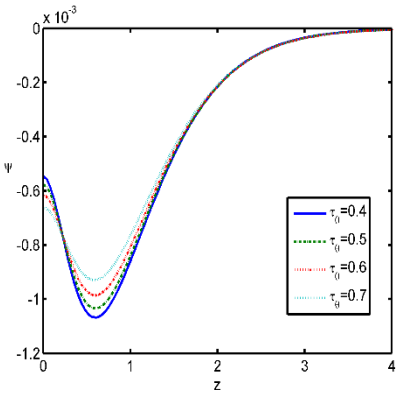

Fig. 15 Distribution of the change in the volume fraction field ψ versus z

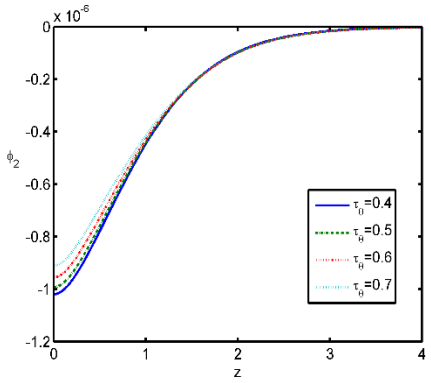

Fig. 16 Distribution of the micro rotation component ϕ_2 versus z

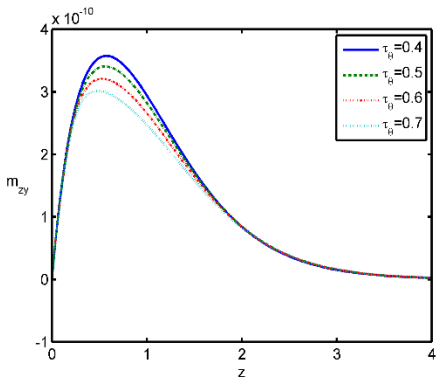

Fig. 17 Distribution of the couple stress tensor component m_{zy} versus z

the volume fraction field ψ, the micro-rotation ϕ_2, the couple stress m_{zy}, the force stress components σ_{zz}, σ_{xz}, the temperature T and the displacement component w against the distance z in the (3PHL) model, for different values of a phase-lag of the heat flux τ_q, namely (τ_q= 0.3, 0.4, 0.6, 0.8), we can see that: the parameter τ_q has significant effects on all the field quantities, the wave has a finite speed of propagation and the (3PHL) model agrees with the generalized thermoelasticity. Fig. 8 shows the distribution of the change in the volume fraction field ψ, against the distance z. It is observed from this figure that the effect of τ_q, is manifest, where the values of the solutions increase with the increase of τ_q, in the range $0 \le z \le 0.3$; while decreasing in the range $0.3 \le z \le 2.4$. Fig. 9 exhibits the distribution of the micro-rotation component ϕ_2, versus z. This figure shows that, the parameter of a phase-lag of the heat flux τ_q has a decreasing effect. Fig. 10 shows the distribution of the couple stress tensor component m_{zy} against the distance z. It is clear that the magnitude of the couple stress tensor component is directly proportional to the parameter m_{zy}, τ_q, increase with the increase of the value while, they in τ_q, for z>0. Fig. 11 displays the distribution of the stress component σ_{zz} versus z. The values of stress component σ_{zz}, increase with the increase of the value τ_q, for z>0. Fig. 12 explains the variation of the stress component σ_{xz} against the distance z; from this figure we see that the values of σ_{xz} decrease with the increase of τ_q in the range $0 \le z \le 0.4$; and increase in the range $0.4 \le z \le 2.5$, while the values of σ_{xz} are the same when $z \ge 2.5$. Fig. 13 exhibits the values of the temperature T against the distance z; this figure shows that, the magnitude of the temperature T is directly proportional to the parameter τ_q, where, they increase with the increase of the value of τ_q, for $z > 0$. Fig. 14 displays the distribution of the displacement component w versus z. It is clear that, the phase-lag of the heat flux τ_q, has a decreasing effect.

6.3 The phase-lag of temperature gradient effect

Figs. 15-21 show the comparisons among the change in the volume fraction field ψ, the micro-rotation ϕ_2, the couple stress m_{zy}, the force stress components σ_{zz}, σ_{xz} the temperature T and the displacement component w against

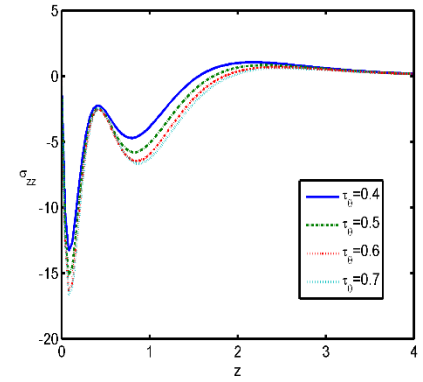

Fig. 18 Distribution of the stress component σ_{zz} versus z

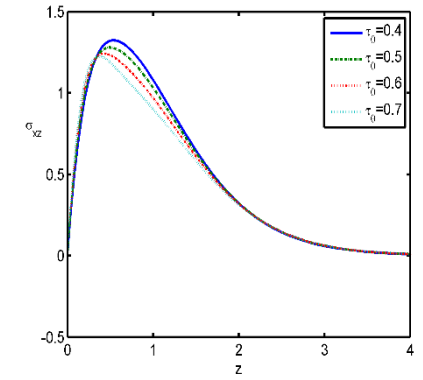

Fig. 19 Distribution of the stress component σ_{xz} versus z

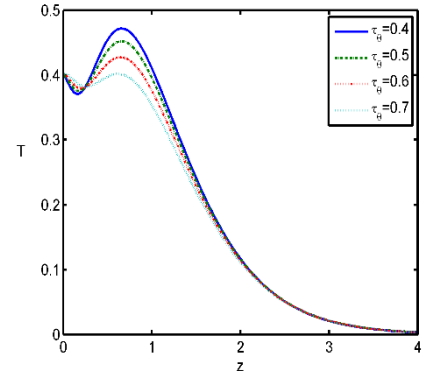

Fig. 20 Distribution of the temperature T versus z

the distance z in the (3PHL) model, for different values

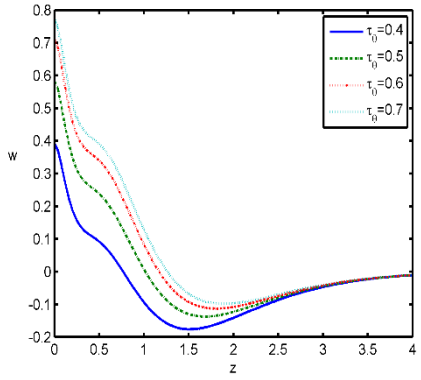

Fig. 21 Distribution of the displacement component w versus z

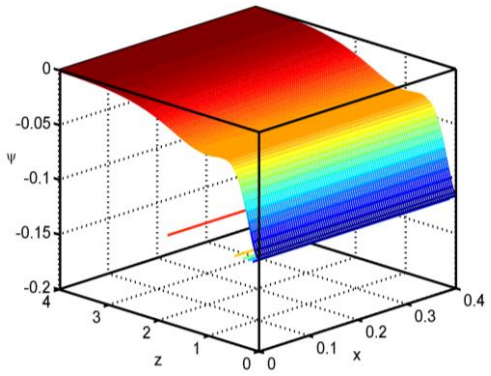

Fig. 22 Three-dimensional curve distribution of the change in the volume fraction field ψ versus the distances

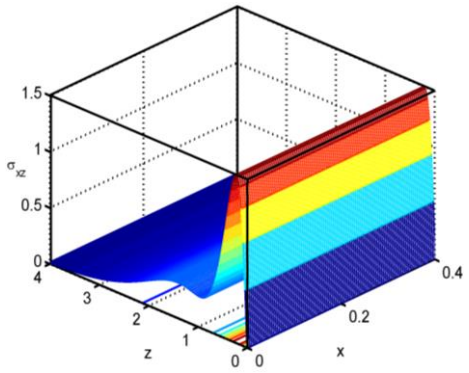

Fig. 23 Three-dimensional curve distribution of the stress component σ_{xz} versus the distances

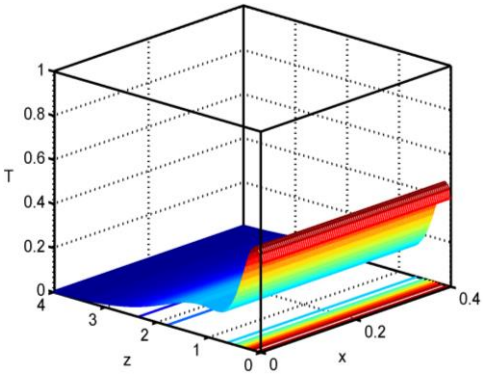

Fig. 24 Three-dimensional curve distribution of the temperature T versus the distances

of a phase-lag of temperature gradient τ_θ, namely τ_θ (τ_θ = 0.4, 0.5, 0.6, 0.7) at Ω=0.3. We can see that: the parameter τ_θ has a significant effect on all the field quantities.

In Figs. 15, 16 and 21 respectively, the magnitude of the change in the volume fraction field ψ the micro-rotation component ϕ_2, and the displacement component w, is directly proportional to the parameter τ_θ, while, they increase with the increase of the value τ_q, for $z > 0$. Figs. 17, 18, 19 and 20 depict the distributions of couple stress tensor component m_{zy}, the stress components σ_{zz}, σ_{xz} and the temperature T in (3PHL) model for various values of τ_θ. It is observed from these figures that the effect of τ_θ, is manifest, where the values of the solutions are increasing with the decrease of τ_θ.

6.4 The 3D surface curves

Figs. 22-24 are giving 3D surface curves for the physical quantities i.e., of the change in the volume fraction field ψ, the stress component σ_{xz} and the temperature T for the effect of rotation on micropolar thermoelastic medium with voids in the context of the (3PHL) model. These figures are very important to study the dependence of these physical quantities on the vertical component of distance.

7. Conclusions

According to the above results, we can conclude that:

- The rotation has an observable effect on the distribution of the physical quantities as shown in the previous analytical solution and discussion.
- The phase-lag of the heat flux parameter and the phase-lag of temperature gradient have a great effect on the distribution of the considered physical quantities.
- The physical quantities are satisfying all the boundary conditions.
- The used method is applicable to a wide range of thermodynamics and thermoelastic problems.
- The obtained results of this article are of great interest in material science and designers of new materials researchers. Moreover, the study of relaxation time and the rotation are useful to improve the conditions of oil extractions and drilling.

Declaration of conflict of interests

The authors declared no potential conflicts of interest with respect to the research, authorship, and/or publication of this article.

Funding

The authors received no financial support for the research, authorship, and/or publication of this article.

References

Abbas, I.A. and Marin M.I. (2017), “Analytical solution of

thermoelastic interaction in a half-space by pulsed laser heating", *Phys. E Low-Dimen. Syst. Nanostruct.*, **87**, 254-260. https://doi.org/10.1016/j.physe.2016.10.048.

Abo-Dahab, SM., Abd-Alla, A.M. and Kilany, A.A. (2019), "Effects of rotation and gravity on an electro-magneto-thermo-elastic medium with diffusion and voids by using the Lord-Shulman and dual-phase-lag models", *Appl. Math. Mech.*, **40**(8), 1135-1154. https://doi.org/10.1007/s10483-019-2504-6.

Al-Basyouni, K.S., Ghandourah, E., Mostafa, H.M. and Algarni, A. (2020), "Effect of the rotation on the thermal stress wave propagation in non-homogeneous viscoelastic body", *Geomech. Eng.*, **21**(1), 1-9. https://doi.org/10.12989/gae.2020.21.1.001.

Arifa, S., Singh, B., Jahangir, A. and Muhammad, N. (2017), "Plane harmonic waves in rotating medium under the effect of micro-temperature and dual-phase-lag thermoelasticity", *UPB Sci. Bull. Ser. D*, **79**(3), 13-25.

Bhatti, M.M., Zeeshan, A., Tripathi, D. and Ellahi, R. (2018), "Thermally developed peristaltic propulsion of magnetic solid practicles in biorheological fluids", *Ind. J. Phys.*, **92**(4), 423-430 https://doi.org/10.1007/s12648-017-1132-x.

Bhatti, M.M., Shahid, A., Abbas, T., Alamri, S.Z. and Ellahi, R. (2020), "Study of activation energy on the movement of gyrotactic microorganism in a magnetized nanofluids past a porous plate", *Processes*, **8**(3), 328-348. https://doi.org/10.3390/pr8030328.

Chandrasekharaiah, D.S. (1987), "Plane waves in a rotating elastic solid with voids", *Int. J. Eng. Sci.*, **25**(5), 591-596. https://doi.org/10.1016/0020-7225(87)90109-1.

Choudhuri, S.K.R. (2007), "On a thermoelastic three phase lag model", *J. Therm. Stress.*, **30**, 231-238. https://doi.org/10.1080/01495730601130919.

Cicco, S.D. and Diaco, M. (2002), "A theory of thermoelastic materials with voids without energy dissipation", *J. Therm. Stress.*, **25**(5), 493-503. https://doi.org/10.1080/01495730252890203.

Dhaliwal, R.S. and Wang, J. (1994), "Domain of influence theorem in the theory of elastic materials with voids", *Int. J. Eng. Sci.*, **32**, 1823-1828. https://doi.org/10.1016/0020-7225(94)90111-2.

Eringen, A.C. (1966), "Linear theory of micropolar elasticity", *J. Math. Mech.*, **15**, 909-924.

Eringen, A.C. (1970), *Foundations of Micropolar Thermoelasticity*, Course of Lectures No. 23, CISM Udine, Springer.

Ellahi, R., Zeeshain, A., Hussain, F. and Abbas, T. (2018), "Study of shiny film coating on multi-fluid flows of a rotating disk suspended with nano-sized silver and gold particles: A comparative analysis", *Coatngs*, **8**(12), 422-448. https://doi.org/10.3390/coatings8120422.

El-Karamany, A.S. and Ezzat, M.A. (2013), "On the three-phase-lag linear micropolar thermoelasticity theory", *Eur. J. Mech. A Solids*, **40**, 198-208. https://doi.org/10.1016/j.euromechsol.2013.01.011.

Hobiny, A.D. and Abbas, I.A. (2020), "Fractional order thermoelastic wave assessment in a two-dimension medium with voids", *Geomech. Eng.*, **21**(1), 85-93. https://doi.org/10.12989/gae.2020.21.1.085.

Iesan, D. (1986), "A theory of thermoelastic materials with voids", *Acta Mech.*, **60**, 67-89. https://doi.org/10.1007/BF01302942.

Itu, C., Öchsner, A., Vlase, S. and Marin, M.I. (2019), "Improved rigidity of composite circular plates through radial ribs", *Proc. Inst. Mech. Eng. Part L J. Mater. Des. Appl.*, **233**(8), 1585-1593. https://doi.org/10.1177/1464420718768049.

Kaddari, M., Kaci, A., Bousahla, A.A., Tounsi, A., Bourada, F., Tounsi, A., Adda Bedia, E.A. and Al-Osta, M.A. (2020), "A study on the structural behaviour of functionally graded porous plates on elastic foundation using a new quasi-3D model: Bending and Free vibration analysis", *Comput. Concrete*, **25**(1), 37-57. https://doi.org/10.12989/cac.2020.25.1.037.

Lata, P. and Kaur, I. (2018a), "Effect of hall current in transversely isotropic magneto-thermoelastic rotating medium with fractional order heat Transfer due to normal force", *Adv. Mater. Res.*, **7**(3), 203-220. https://doi.org/10.12989/amr.2018.7.3.203.

Lata, P. and Kaur, I. (2018b), "Effect of inclined load on transversely isotropic magneto thermo-elastic rotating solid with time harmonic source", *Adv. Mater. Res.*, **8**(2), 83-102. https://doi.org/10.12989/amr.2019.8.2.083.

Lata, P. and Singh, S. (2019), "Effect of nonlocal parameter on nonlocal thermoelastic solid due to inclined load", *Steel Compos. Struct.*, **33**(1), 123-131. https://doi.org/10.12989/scs.2019.33.1.123.

Marin, M. (1998), "A temporally evolutionary equation in elasticity of micropolar bodies with voids", *Bull. Ser. A Appl. Math. Phys.*, **60**, 3-12.

Marin, M.I. and Nicaise, S. (2016), "Existence and stability results for thermoelastic dipolar bodies with double porosity", *Contin. Mech. Thermodyn.*, **28**(6), 1645-1657. https://doi.org/10.1007/s00161-016-0503-4.

Marin, M.I., Ellahi, R. and Chirilă, A. (2017), "On solutions of Saint-Venant's problem for elastic dipolar bodies with voids", *Carpathian J. Math.*, **33**(2), 219-232.

Marin, M.I., Vlase, S., Ellahi, R. and Bhatti, M.M. (2019), "On the partition of energies for the backward in time problem of thermoelastic materials with a dipolar structure", *Symmetry*, **11**(7), 863. https://doi.org/10.3390/sym11070863.

Mirzaei, M.M.H., Arefi, M. and Loghman, A. (2019), "Creep analysis of a rotating functionally graded simple blade: Steady state analysis", *Steel Compos. Struct.*, **33**(3), 463-472. https://doi.org/10.12989/scs.2019.33.3.463.

Nunziato, J.W. and Cowin, S.C. (1979), "A nonlinear theory of elastic materials with voids", *Arch. Rational Chanics and Anal.*, **72**(2) 175-201. https://doi.org/10.1007/BF00249363.

Othman, M.I.A., Hasona, W.M. and Eraki, E.E.M. (2014), "The effect of initial stress on generalized thermoelastic medium with three-phase-lag model under temperature dependent properties", *Can. J. Phys.*, **92**(5), 448-457. https://doi.org/10.1139/cjp-2013-0461.

Othman, M.I.A., Hasona, W.M. and Abd-Elaziz, E.M. (2015), "Effect of rotation and initial stress on generalized micropolar thermoelastic medium with three-phase-lag", *J. Comput. Theor. Nanosci.*, **12**(9), 2030-2040. https://doi.org/10.1166/jctn.2015.3983.

Othman, M.I.A. and Eraki, E.E.M. (2017), "Generalized magneto-thermoelastic half space with diffusion under initial stress using three-phase-lag model", *Mech. Based Des. Struct. Mach.*, **45**(2), 145-159. http://doi.org/10.1080/15397734.2016.1152193.

Othman, M.I.A., Said, S.M. and Marin, M. (2019), "A novel model of plane waves of two-temperature fiber-reinforced thermoelastic medium under the effect of gravity with three-phase-lag model", *Int. J. Numer. Meth. Heat Fluid Flow*, **29**(12), 4788-4806. http://doi.org/10.1108/HFF-04-2019-0359.

Puri, P. and Cowin, S.C. (1985), "Plane waves in linear elastic materials with voids", *J. Elast.*, **15**, 167-185. https://doi.org/10.1007/BF00041991.

Quintanilla, R. and Racke, R. (2008), "A note on stability in three-phase-lag heat conduction", *Int. J. Heat Mass Transfer*, **51**, 24-29. https://doi.org/10.1016/j.ijheatmasstransfer.2007.04.045.

Scarpetta, E. (1995), "Well posedness theorems for linear elastic materials with voids", *Int. J. Eng. Sci.*, **33**(2), 151-161. https://doi.org/10.1016/0020-7225(94)00060-W.

Schoenberg, M. and Censor, D. (1973), "Elastic waves in rotating media", *Quart. Appl. Math.*, **31**, 115-125. https://doi.org/10.1090/qam/99708.

Shahid, A., Huang, H., Bhatti, M.M., Zhang, L. and Ellahi, R.

(2020), "Numerical investigation on the swimming of gyrotactic microorganisms in nanofluids through porous medium over a stretched surface", *Mathematics*, **8**(3), 380-397. https://doi.org/10.3390/math8030380.
Sur, A. and Kanoria, M. (2014), "Thermoelastic interaction in a viscoelastic functionally graded half-space under three-phase-lag model", *Eur. J. Comput. Mech.*, **23**(5-6), 179-198. https://doi.org/10.1080/17797179.2014.978143.
Sur, A. and Kanoria, M. (2015), "Three-phase-lag elasto-thermo-diffusive response in an elastic solid under hydrostatic pressure", *Int. J. Adv. Appl. Math. Mech.*, **3**(2), 121-137.
Tzou, D.Y. (1995), "A unified field approach for heat conduction from macro to micro scales", *J. Heat Transf.*, **117**, 8-16. https://doi.org/10.1115/1.2822329.

GC

Nomenclature

λ, μ	The Lamé constants
ρ	The material density
j	Microinertia
τ_q	The phase-lag of heat flux
T_0	The reference temperature
$\boldsymbol{\varphi}$	Micro rotation vector
x, y, z	The Cartesian coordinates variables
t	The time variable
α_t	The coefficient of linear thermal expansion
e	Dilatation
m_{ij}	Couple stress tensor components
σ_{ij}	Stress tensor components
ψ	Change in volume fraction field
ε_{ij}	Strain tensor components
K	The additional material constant
F_i	Body force
C_e	The specific heat at constant strain
δ_{ij}	Kronecker delta
K^*	Thermal conductivity
ε_0	Electric permeability
μ_0	Magnetic permeability
$\boldsymbol{\Omega}$	Angular velocity
τ_θ	The phase-lag of temperature gradient
∇^2	Laplace operator
υ	The volume thermal expansion Permutation tensor ε_{ijr}
τ_v	Phase lag of thermal displacement gradient
τ_q	Phase lag of heat flux
k, α, β, γ	The material constants due to presence of micropolar
$\alpha^*, \eta^*, \omega^*, \beta^*, m, \xi^*$	The material constants due to presence of voids
$\boldsymbol{u}$	The displacement vector, $\boldsymbol{u} \equiv (u, v, w)$, u, v and w are the displacement components
T	Absolute temperature (temperature above the reference temperature T_0) such that $\left\|(T - T_0)/T_0\right\| << 1$

Appendix A

$$a_1=\frac{\beta^*}{\rho c_1^2},\quad a_2=(\frac{\mu+k}{\rho c_1^2}),\quad a_3=\frac{k}{\rho c_1^2},\quad a_4=K^*(1+\tau_v s),$$

$$a_5=K\omega(1+\tau_\theta s),\ a_7=\rho c_e c_1^2 s^2,\quad a_6=(1+\tau_q s+\frac{1}{2}\tau_q^2 s^2),$$

$$a_8=\frac{\upsilon^2 T_0}{\rho},\quad a_9=\frac{m\upsilon T_0}{\rho\omega},\quad a_{10}=\frac{\rho j c_1^2}{\gamma},\quad a_{11}=\frac{kc_1^2}{\gamma\omega^2},$$

$$a_{12}=\frac{\rho\xi^* c_1^2}{\alpha^*},\ a_{13}=\frac{\omega^* c_1^2}{\omega\alpha^*},\ a_{14}=\frac{\eta^* c_1^2}{\alpha^*\omega^2},\ a_{15}=\frac{\beta^* c_1^4}{\alpha^*\omega^4},$$

$$a_{16}=\frac{m\rho c_1^4}{\alpha^*\omega^2\upsilon},\quad a_{17}=\frac{2\mu+k}{\rho c_1^2},\quad a_{18}=\frac{\lambda}{\rho c_1^2},\ a_{19}=\frac{\mu}{\rho c_1^2},$$

$$a_{20}=\frac{\gamma\omega^2}{\rho c_1^4},\quad a_{21}=\frac{\beta\omega^2}{\rho c_1^4}.\quad b_1=a^2+s^2-\Omega^2,\quad b_2=2\Omega\mathrm{s},$$

$$b_3=a_2a^2+s^2-\Omega^2,\quad b_4=a_4+a_5s,\quad b_5=b_4a^2+a_6a_7,$$

$$b_6=a_6a_8s^2,\quad b_7=b_6a^2,\quad b_8=a_6a_9s,\quad b_9=a^2+a_{10}s^2+2a_{11},$$

$$b_{10}=a_{11}a^2,\quad b_{11}=a^2+a_{12}s^2+a_{13}s+a_{14},\quad b_{12}=a_{15}a^2.$$

Appendix B

$$A=\frac{1}{a_2b_4}[-a_2b_5-a_2b_6-b_3b_4+a_3a_{11}b_4-a_2b_1b_4-a_2b_4b_9$$
$$-a_2b_4b_{11}+a_1a_2a_{15}b_4],$$
$$\mathrm{D}=\frac{\mathrm{d}}{\mathrm{dz}},$$

$$B=\frac{1}{a_2b_4}[b_2^2b_4+a_2b_7+b_3b_5+b_3b_6-a_3a_{11}b_5-a_3a_{11}b_6-a_2a_{15}b_8$$
$$+a_2a_{16}b_8+a_2b_1b_5+a_2b_5b_6-a_3b_4b_{10}b_9+a_2b_6b_9+a_2b_5b_{11}$$
$$+a_2b_6b_{11}+b_1b_3b_4+b_3b_4b_9+b_3b_4b_{11}-a_1a_2a_{15}b_5-a_1a_2a_{16}b_6$$
$$-a_1a_2b_4b_{12}-a_3a_{11}b_1b_4-a_1a_{15}b_3b_4-a_3a_{11}b_4b_{11}+a_2b_1b_4b_9$$
$$+a_2b_1b_4b_{11}+a_2b_4b_9b_{11}+a_1a_3a_{11}a_{15}b_4-a_1a_2a_{15}b_4b_9],$$

$$C=\frac{1}{a_2b_4}[-b_2^2b_5-b_3b_7+a_3a_{11}b_7-a_2b_7b_9+a_3b_5\,\mathrm{b}_{10}+a_3b_6b_{10}$$
$$-a_2b_7b_{11}+a_2b_8b_{12}+a_{15}b_3b_8-a_{16}b_3b_8-b_1b_3b_5$$
$$-b_3b_5b_9-b_3b_6b_9-b_3b_5b_{11}-b_3b_6b_{11}-b_2^2b_4b_9-b_2^2b_4b_{11}$$
$$+a_1a_2a_{16}b_7-a_3a_{11}a_{15}b_8+a_3a_{11}a_{16}b_8+a_1a_2b_5b_{12}+a_3a_{11}b_1b_5$$
$$+a_1a_{15}b_3b_5+a_1a_{16}b_3b_6-a_2a_{16}b_1b_8+a_3a_{11}b_5b_{11}$$
$$+a_3a_{11}b_6b_{11}+a_2a_{15}b_8b_9-a_2a_{16}b_8b_9-a_2b_1b_5b_9$$
$$+a_3b_1b_4b_{10}-a_2b_1b_5b_{11}+a_1b_3b_4b_{12}-a_2b_5b_9b_{11}$$
$$-a_2b_6b_9b_{11}+a_3b_4b_{10}b_{11}-b_1b_3b_4b_9-b_1b_3b_4b_{11}-b_3b_4b_9b_{11}$$
$$-a_1a_3a_{11}a_{15}b_5-a_1a_3a_{11}a_{16}b_6-a_1a_3a_{11}b_4b_{12}+a_1a_2a_{15}b_5b_9$$
$$-a_1a_3a_{15}b_4b_{10}+a_1a_2a_{16}b_6b_9+a_1a_2b_4b_9b_{12}+a_3a_{11}b_1b_4b_{11}$$
$$+a_1a_{15}b_3b_4b_9-a_2b_1b_4b_9b_{11}],$$

$$E=\frac{1}{a_2b_4}[-a_3b_7b_{10}+b_3b_7b_9+b_3b_7b_{11}-b_3b_8b_{12}+a_{16}b_2^2b_8$$
$$+b_2^2b_5b_9+b_2^2b_5b_{11}-a_1a_{16}b_3b_7-a_3a_{11}b_7b_{11}+a_3a_{11}b_8b_{12}$$
$$+a_3a_{15}b_8b_{10}-a_3a_{16}b_8b_{10}-a_3b_1b_5b_{10}-a_1b_3b_5b_{12}$$
$$+a_{16}b_1b_3b_8+a_2b_7b_9b_{11}-a_3b_5b_{10}b_{11}-a_3b_6b_{10}b_{11}$$
$$-a_2b_8b_9b_{12}-a_{15}b_3b_8b_9+a_{16}b_3b_8b_9+b_1b_3b_5b_9$$
$$+b_1b_3b_5b_{11}+b_3b_5b_9b_{11}+b_3b_6b_9b_{11}+b_2^2b_4b_9b_{11}$$
$$+a_1a_3a_{11}a_{16}b_7+a_1a_3a_{11}b_5b_{12}+a_1a_3a_{15}b_5b_{10}-a_1a_2a_{16}b_7b_9$$
$$+a_1a_3a_{16}b_6b_{10}-a_3a_{11}a_{16}b_1b_8-a_1a_2b_5b_9b_{12}$$
$$+a_1a_3b_4b_{10}b_{12}-a_3a_{11}b_1b_5b_{11}-a_1a_{15}b_3b_5b_9-a_1a_{16}b_3b_6b_9$$
$$+a_2a_{16}b_1b_8b_9+a_2b_1b_5b_9b_{11}-a_1b_3b_4b_9b_{12}-a_3b_1b_4b_{10}b_{11}$$
$$+b_1b_3b_4b_9b_{11}],$$

$$F=\frac{1}{a_2b_4}[-\mathrm{a}_{16}b_2^2b_8b_9-b_2^2b_5b_9b_{11}+\mathrm{a}_3b_7b_{10}b_{11}-\mathrm{a}_3b_8b_{10}b_{12}$$
$$-b_3b_7b_9b_{11}+b_3b_8b_9b_{12}-a_1a_3a_{16}b_7b_{10}-a_1a_3b_5b_{10}b_{12}$$
$$+a_1a_{16}b_3b_7b_9+a_3a_{16}b_1b_8b_{10}+a_1b_3b_5b_9b_{12}+a_3b_1b_5b_{10}b_{11}$$
$$-a_{16}b_1b_3b_8b_9-b_1b_3b_5b_9b_{11}],$$

$$H_{1n}=\frac{b_2(k_n^2-b_9)}{(k_n^2-b_9)(\mathrm{a}_2k_n^2-b_3)-a_3(\mathrm{a}_{11}k_n^2-b_{10})},$$

$$H_{2n}=\frac{(k_n^2-b_{11})(\mathrm{b}_6k_n^2-b_7)-b_8(\mathrm{a}_{15}k_n^2-b_{12})]}{(k_n^2-b_{11})(\mathrm{b}_4k_n^2-b_5)-b_8a_{16}},$$

$$H_{3n}=\frac{b_2(\mathrm{a}_{11}k_n^2-b_{10})}{-a_3(\mathrm{a}_{11}k_n^2-b_{10})-(\mathrm{a}_2k_n^2-b_3)(k_n^2-b_9)},$$

$$H_{4n}=\frac{a_{16}(\mathrm{b}_6k_n^2-b_7)-(\mathrm{b}_4k_n^2-b_5)(\mathrm{a}_{15}k_n^2-b_{12})}{-a_{16}b_8-(\mathrm{b}_4k_n^2-b_5)(k_n^2-b_{11})}.$$

$$S_{1i}=-a_{17}(a^2+iak_nH_{1n})+a_{18}(k_n^2-a^2)+a_1H_{4n}-H_{2n},\quad \mathrm{i}=1,2,3,4,5$$

$$S_{2i}=a_{18}(k_n^2-a^2)+a_1H_{4n}-H_{2n},\quad i=1,2,3,4,5$$

$$S_{3i}=a_{19}k_n^2H_{1n}-ia(a_2+a_{19})k_n+a_2a^2H_{1n}+a_3H_{3n},\quad i=1,2,3,4,5$$

$$S_{4i}=a_{17}(k_n^2+iak_nH_{1n})+a_{18}(k_n^2-a^2)+a_1H_{4n}-H_{2n},\quad i=1,2,3,4,5$$

$$S_{5i}=a_2k_n^2H_{1n}-ia(a_2+a_{19})k_n+a_{19}a^2H_{1n}-a_3H_{3n},\quad i=1,2,3,4,5$$

$$S_{6i}=iaa_{20}H_{3n}M_n,\quad i=1,2,3,4,5$$
$$S_{7i}=-a_{20}k_nH_{3n},\quad i=1,2,3,4,5$$
$$S_{8i}=iaa_{21}H_{3n},\quad i=1,2,3,4,5$$
$$S_{9i}=-a_{21}k_nH_{3n},\ i=1,2,3,4,5$$